



Coral-like porous composite material of silicon and carbon synthesized by using diatomite as self-template and precursor with a good performance as anode of lithium-ions battery



Fang Di ^{a, b}, Ning Wang ^{a, c}, Lixiang Li ^{a, b, **}, Xin Geng ^{a, b}, Haiming Yang ^{a, b}, Weimin Zhou ^{a, b}, Chengguo Sun ^{a, b}, Baigang An ^{a, b, *}

^a School of Chemical Engineering, University of Science and Technology Liaoning, 185 Qianshanzhong Road, Anshan, 114051, China

^b Key Laboratory of Energy Materials and Electrochemistry Research Liaoning Province, University of Science and Technology Liaoning, 185 Qianshanzhong Road, Anshan, 114051, China

^c School of Chemical Engineering, University of Tianjin, 92 Weijin Road, Tianjin, 300072, China

ARTICLE INFO

Article history:

Received 26 August 2020

Received in revised form

15 September 2020

Accepted 16 September 2020

Available online 18 September 2020

Keywords:

Lithium-ion battery

Silicon

Diatomite

Hierarchical pores

Volumetric effects

ABSTRACT

Developing silicon based anode of lithium-ion battery (LIB) is seriously blocked by the huge volume change of lithiation and delithiation and the corresponded high cost paying to solve it, although Si with the theoretical capacity of 4200 mAh g⁻¹ for Li⁺ storage. In this study, natural diatomite with low cost was using as precursor and self-template to produce Si and construct porous structure, a coral-like porous Si/C (CLP-Si/C) material has been successfully synthesized through the NaCl added magnesiothermic reduction reaction (MRR) technology and acetylene CVD method. The hierarchical structure of macro-/mesopores in CLP-Si/C are inherited from diatomite itself and produced by removing the unreacted SiO₂ in diatomite and the byproduct of MgO of MRR. Acetylene CVD further constructs a shell-core structure of carbon layers and Si particles. The hierarchical pores and core-shell structure make CLP-Si/C exhibit a stable cycling performance as LIB anode that the capacity of 990.6 mAh g⁻¹ can be kept after 100 cycles at a rate of 250 mA g⁻¹. This work provides a simple, low-cost and scalable strategy for producing porous Si/C anode materials with high-performance by using diatomite as both precursor and template, and is promising in the development of practical application of Si based anode materials of lithium-ion battery.

© 2020 Elsevier B.V. All rights reserved.

1. Introduction

To meet the global energy and environmental demands, tremendous efforts have been devoted to develop those renewable energy systems such as wind and solar powers, however, which are largely limited by intermittent energy production due to the factors of weather and locations [1]. Therefore, their efficient utilization requires energy storage devices for powers transfer [2,3]. Rechargeable lithium-ion battery (LIB) is a much popular energy storage device due to its high energy density, high voltage and

environmental friendliness and has been widely used in electronic devices, electric vehicles and power stations [4]. The reversible storage capacity of commercial LIB is limited by the electrode materials. Presently, the most commonly used anode materials of LIB is graphite with a theoretical capacity of 372 mAh g⁻¹ on the basis of the mechanism of Li⁺ storage, however, it can't meet requirements of quick developments of electric automobile [5].

To significantly increase the energy density of anode of LIB, the anode materials of energy storage by alloying and dealloying of lithium are highly promising owing to a large energy density of these materials [6]. Among them, silicon has the highest theoretical capacity of lithium ion storage up to 4200 mAh g⁻¹ [7]. Si has also some advantages of becoming an anode material for commercial LIBs. It is the second abundant element in the earth's crust, low in cost, and harmless to the environment. The voltage platform of silicon is slightly higher than graphite, which can improve the safety of LIBs through avoiding lithium dendrites and surface

* Corresponding author. School of Chemical Engineering, University of Science and Technology Liaoning, 185 Qianshanzhong Road, Anshan, 114051, China.

** Corresponding author. Key Laboratory of Energy Materials and Electrochemistry Research Liaoning Province, University of Science and Technology Liaoning, 185 Qianshanzhong Road, Anshan, 114051, China.

E-mail addresses: lxli2005@126.com (L. Li), bgan@ustl.edu.cn (B. An).

lithium plating [8]. Despite these advantages, the development of silicon anodes of LIBs is still hampered by their poor cycling performance caused by the severe volume changes of Si up to 300% during lithiation and delithiation. As a result, the mechanical stress resulted by the volume change of Si anode causes the cracking and pulverization of anode materials and thus the active materials are disconnected from the current collector, resulting in destruction of the conductive network, which leads to rapid capacity fading of LIBs [9,10].

To solve the above problems, many achieved efforts have been reported from the aspects of nanosizing and nanostructuring silicon to minimize the volumetric stress [11,12], preparing the composite materials of Si and carbonaceous materials to alleviate volumetric stress and improve conductivity [13,14] and constructing redundant space for the inflation of silicon lithiation [15,16]. Or these aspects were combined to pursue the Si anode with the better performance. However, one of the most concerned factors limiting commercialization of Si anode that the costs have not yet been paid enough attention and efforts in most of works related to Si anodes.

Silicon is second abundant elements in earth crust and thus directs utilizing natural sources containing Si to synthesize Si anode materials of LIBs is highly expecting for lowering the cost and accelerating commercialization of Si based anode of LIBs. SiO₂ are generally used as the precursor for producing Si and SiC anode [17,18]. Diatomite as natural resource has a big reserve and contains bulk phase of SiO₂. In this work, diatomite was used as the precursor and self-template to synthesize a coral-like porous Si/C (CLP-Si/C) owning mesoporous and macroporous structure. The CLP-Si/C anode owns the macropores inheriting from the intrinsic pores of diatomite and the macro-/mesopores formed by removing of the unreacted SiO₂ of diatomite and byproduct of MgO after MRR. Both the macropores and mesopores are constructed through utilizing the structure and composition of diatomite without using any additional template. As anode of LIB, the resultant CLP-Si/C exhibits a good performance with capacitance of 990.6 mAh g⁻¹ at the current density of 250 mA g⁻¹ after 100 cycles.

2. Experimental

2.1. Materials preparation

First, 0.50 g of diatomite (DE) powder (AR, Tianjin, Zhiyuan), 0.30 g of magnesium powder (CR, Shanghai, Aladdin) and 5.00 g of NaCl powder (AR, Shanghai, Sinopharm Chemical Reagent) were ground and mixed together using an agate mortar for 20 min. The obtained DE-Mg-NaCl mixture was placed in a quartz-tube furnace and purged with pure argon gas. The furnace was heated to 700 °C with a ramp of 5 °C min⁻¹ and then the temperature was held for 4 h. The furnace was naturally cooled in argon atmosphere to ambient temperature. The resultant product was firstly washed several times with deionized water to solve and remove the NaCl. Then the sample was soaked in 6 wt% HCl solution for 10 h to remove the MgO byproduct of MRR, after which the sample was washed by deionized water and dried at 80 °C under vacuum. The main product of MRR after the post treatment was coated the carbon by carrying acetylene CVD as follows. A certain amount of powdered sample was loaded in a ceramic boat and then placed in a horizontal furnace with a flow of argon gas of 80 sccm. The temperature of furnace was heated to 800 °C with a ramp of 25 °C min⁻¹ and then acetylene was immediately flowed into the furnace with a flow of 20 sccm for 30 min. After the furnace was cooled to ambient temperature, the powder sample was taken out and then immersed in 5 wt% HF solution at room temperature for 10 h to remove the residual SiO₂ in the sample. Finally, porous Si/C materials using diatomite as the precursor and the self-template was

obtained, whose synthesis route is shown in Fig. 1 of the schematic diagram.

2.2. Sample characterization

The composition of samples was characterized by using a high-resolution X-ray diffractometer (XRD, Rigaku X'pert Powder, D/MAX-2500×, Cu Kα) and a laser Raman spectroscopy with a wavelength of 532 nm. The microstructure and morphology of samples were observed by using a field-emission scanning electron microscope (SEM, FEI Apreo, operated at 5 kV) and a high-resolution transmission electron microscope (HRTEM, FEI Talos F200×, operated at 200 kV). The specific surface area (SSA) and porosity of sample were characterized by Brunauer-Emmett-Teller analysis (BET, Micromeritics, ASAP2020). In addition, the supplementary study of the Si content of sample was assessed by thermogravimetry (TG, TA Instruments, SDTQ600).

2.3. Electrochemical tests

60 wt% of active material (CLP-Si/C), 20 wt% of Super P, 20 wt% of CMC and appropriate deionized water were weighed and mixed to form a slurry. The mixed slurry was coated on copper foil and then dried in vacuum to prepare an anode plate, which was cut into the disks with diameter of 12 mm. Loading amount of active material onto each anode is about 1.0 mg cm⁻². Half-cells were assembled in a glove box in Ar atmosphere, in which the disk containing CLP-Si/C, a lithium foil, polypropylene membrane (Celgard), and 1.0 mol L⁻¹ LiPF₆ dissolved of ethylene carbonate (EC): dimethyl carbonate (DC) = 1:1 were used as working electrode, counter/reference electrode, separator and electrolyte, respectively. Galvanostatic charge-discharge tests were carried out by using a battery test system (LANHE CT3100) in the voltage range of 0.01–1.5 V vs. Li/Li⁺. In addition, cyclic voltammetry (CV) tests were performed by using a Gamry-3000 electrochemical workstation at a scan rate of 0.05 mV s⁻¹.

3. Results and discussion

Fig. 2a shows the XRD patterns of samples. The bulk phase of diatomite is SiO₂ characterized by prominent peaks around 21.8°, 28.3°, 31.1° and 35.9° corresponding to the crystal face of 101, 111, 102 and 200 (JCPDS76-0940), respectively. After MRR and remove of MgO by HCl solution, the peaks corresponding to the cubic Si face of 111, 220, 311 and 400 can be discerned for the sample (JCPDS 26-1481). It still contains SiO₂ phase in the sample since the inadequate amount of magnesium was used in MRR of diatomite. This sample containing Si and SiO₂ was further coated with carbon by acetylene CVD, and then HF solution was used to remove the phase of SiO₂ for producing pores in the resultant CLP-Si/C anode. The peaks of SiO₂ disappear and the characteristic peaks of Si are clearly observed for the obtained sample. Carbon phase in the sample can't be discerned since its weak intensity compared to Si, however, the subsequent Raman and TEM characterizations is going to confirm the existence of amorphous carbon layers around Si particles.

In the MRR process of diatomite, the additional NaCl component plays an important role on preparation of CLP-Si/C despite it does not attend MRR. In order to clarify the role of NaCl, another experiment of MRR of diatomite without adding NaCl was carried out and the sample also experienced the post-treatments of HCl and HF solution. As the XRD pattern shown, the distinct peaks of Mg₂SiO₄ can be seen even after HF solution treatment, the result confirms that NaCl additive is especially important to avoid the formation of byproduct of Mg₂SiO₄ difficult to be removed. Owing

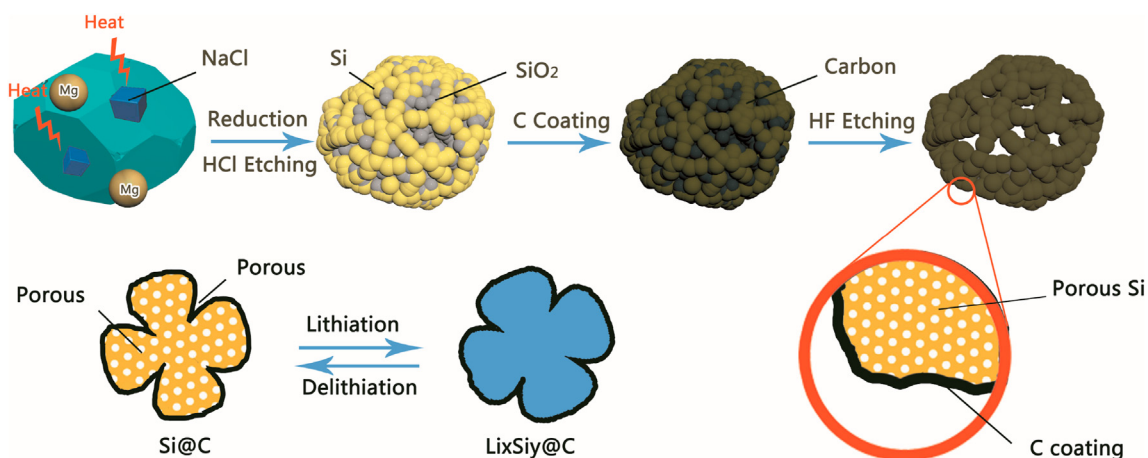


Fig. 1. Schematic diagram of preparing the coral-like porous Si/C (CLP-Si/C).

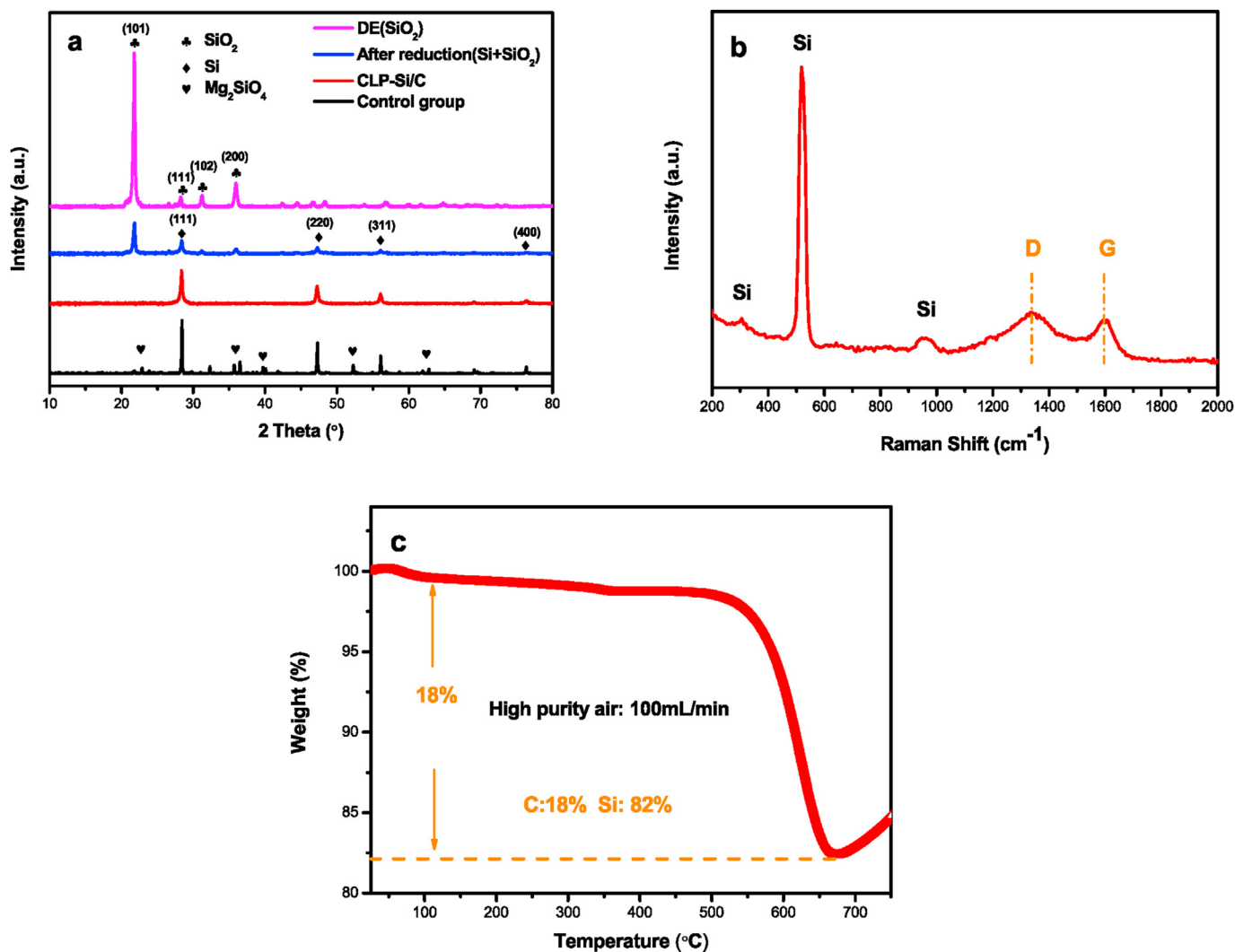


Fig. 2. (a) XRD patterns of diatomite before and after MRR; (b) the Raman spectrum of the CLP-Si/C sample; (c) TG curve of the CLP-Si/C sample.

to the exothermic nature of MRR ($\text{SiO}_2 + \text{Mg} \rightarrow \text{Si} + \text{MgO}$ $\Delta H = -546.42 \text{ kJ mol}^{-1}$) [18], the local temperature of furnace chamber is most probably higher than the given temperature of

700 °C, which can cause the formation of Mg_2SiO_4 by the side reaction of MgO and SiO_2 when temperature is higher than 850 °C. Since the melting point of pure NaCl is 804 °C, NaCl can act as a heat

scavenger to avoid the side reaction occurring at the higher temperature through the endothermic process of melting NaCl during the MRR.

Fig. 2b shows the Raman spectra of CLP-Si/C sample. The sharp peak at 518 cm^{-1} and another two weak peaks at 306 cm^{-1} and 948 cm^{-1} are corresponding to the characteristic peaks of crystalline Si [21,22]. The presence of the peaks at 1339 cm^{-1} and 1593 cm^{-1} in the Raman spectrum (referred as the D-band and G-band of carbon, respectively) confirms the existence of the carbon layers. The I_D/I_G value of 1.11 also reflects the low graphitic degree in the carbon layers. The presence of the carbon layers can improve the electrical conductivity of the anode and strengthen the structural strength of the composite material and thus could improve cycle stability of anode. In addition, the Si content of CLP-Si/C determined by thermogravimetry (TG) is shown in Fig. 2c, which is about 82%.

Fig. 3 shows the SEM images of samples. The pure diatomite looks like a round sieve with many uniform distributed circular pores with size around several hundreds of nanometers. After the MRR and HCl solution treatment, the obtained sample appears the morphology of small particles fused together and there are still some macropores inheriting from diatomite, but there also many new formed pores between the small particles, probably which are produced by the removal of byproduct of MgO. After acetylene CVD, it is more clearly to observe those small particles fused together and the pores since the enhanced conductivity by carbon layers. After HF solution treatment, the final product of CLP-Si/C exhibits a coral-like morphology that many small particles fused connection and there are many cavities with different depth between the fused particles resulted by the remove of the unreacted SiO_2 .

HRTEM was used to further observe microstructure of CLP-Si/C. The carbon layers with the thickness of about 10 nm around Si particles can be observed and there are some space between the carbon layer and Si particles to construct a shell-core structure of the carbon-coated silicon particles as shown in Fig. 4a and b. In the silicon particles inside carbon shells, many pores with the size of about several tens of nanometers can be also seen, which could be produced by the removal of MgO and SiO_2 as shown in Fig. 4b. Moreover, by the HRTEM with a larger magnification (Fig. 4c) the smaller particle structures can be observed and there are obvious mesoporous channels among them, which can be attributed to

MRR to produce visible mesopores (2–50 nm). In this image, the size of the finally reduced silicon nanoparticles (SiNPs) can be confirmed to be around 10 nm, the particle has obvious lattice fringes corresponding to the 111 crystal plane of Si (Fig. 4d). It was reported that the critical dimension of fracturing of Si lithiation is about 150 nm, below which Si nanoparticles have the toughness enough to endure Si lithiation repeatedly without fracturing [23]. The CLP-Si/C prepared by MRR of diatomite owns not only porous structure to alleviate the volumetric effect but also has good toughness to prevent Si from fracture during Si lithiation and delithiation. Therefore, CLP-Si/C is expecting for using anode materials of LIB.

N_2 adsorption-desorption isotherms of samples were measured and used to analyze the SSA and pore size related parameters, the results are shown in Fig. 5a. Diatomite has only $5.84\text{ m}^2\text{ g}^{-1}$ since it contains only a few of macropores as shown in SEM images (Fig. 3a). However, CLP-Si/C has the obvious adsorption capacity in the all relative pressure. A hysteresis loop in the range of middle-high pressure suggests the mesoporous and macroporous structure of material. Pore size distribution (PSD) curve shown by Fig. 5b further confirms the hierarchical pore consisting of meso- and macropores. Pores of CLP-Si/C are mainly focused on size of 3.1, 9.2, 15.0, 26.9, 37.0, 52.7 and 68.3 nm, respectively. According to the process of preparing CLP-Si/C, these hierarchical pores most derive from diatomite itself including the macropores of diatomite and the new produced meso-/macro-pores through removing the unreacted SiO_2 in the diatomite and byproduct of MgO of MRR. Abundant pores bring CLP-Si/C a large SSA and a high pore volume as listed in Table 1. CLP-Si/C has a SSA of $359.09\text{ m}^2\text{ g}^{-1}$ and a high pore volume of $0.7436\text{ cm}^3\text{ g}^{-1}$ that is much larger than the pristine diatomite of $5.84\text{ m}^2\text{ g}^{-1}$ and $0.0023\text{ cm}^3\text{ g}^{-1}$, respectively. A large SSA of CLP-Si/C could supplies more electrochemical reaction sites facilitating the lithiation and delithiation [24,25]. Abundant and hierarchical pores in CLP-Si/C could efficiently accommodate the volumetric change and bring a good cycling stability when using as anode of LIB.

The electrochemical performance of CLP-Si/C anode of LIB was tested by CV and galvanic charge-discharge technology. Fig. 6a shows the potential profiles of CLP-Si/C electrodes at a rate of 250 mA g^{-1} for 1st, 2nd, 10th, 50th and 100th cycles in the voltage window of 0.01–1.5 V vs. Li/Li^+ electrode. The initial discharge and

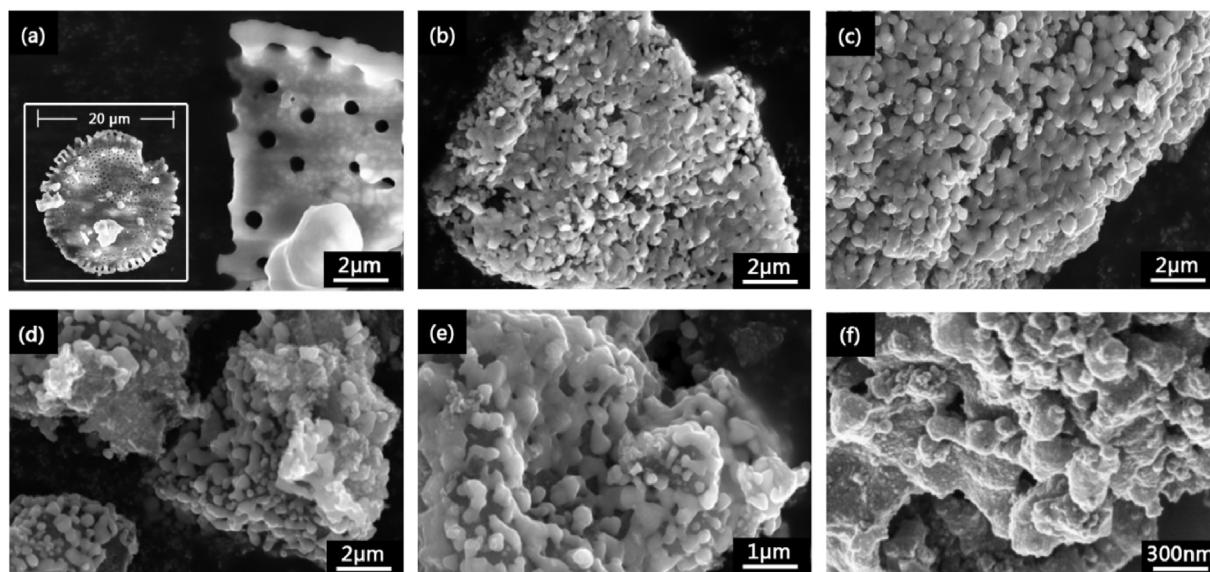


Fig. 3. SEM images of the (a) diatomite; (b) reduction products of diatomite (SiO_2+Si); (c) carbon-coated reduction product; (d)–(f) CLP-Si/C at different magnifications.

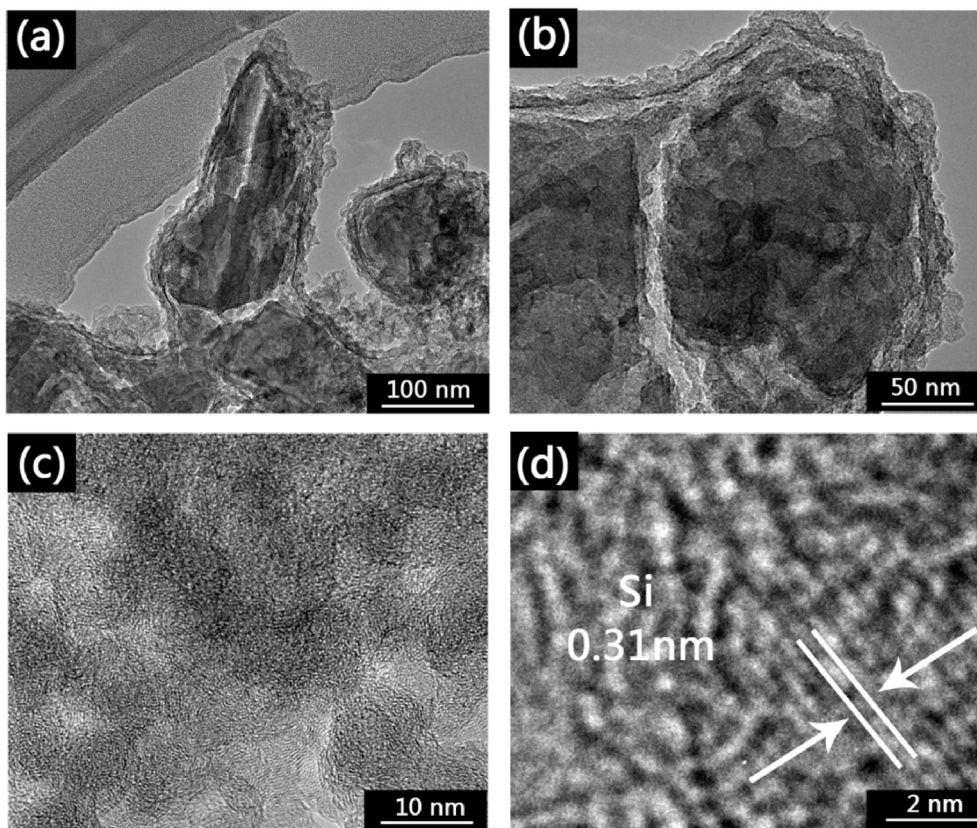


Fig. 4. TEM images of CLP-Si/C at different magnifications.

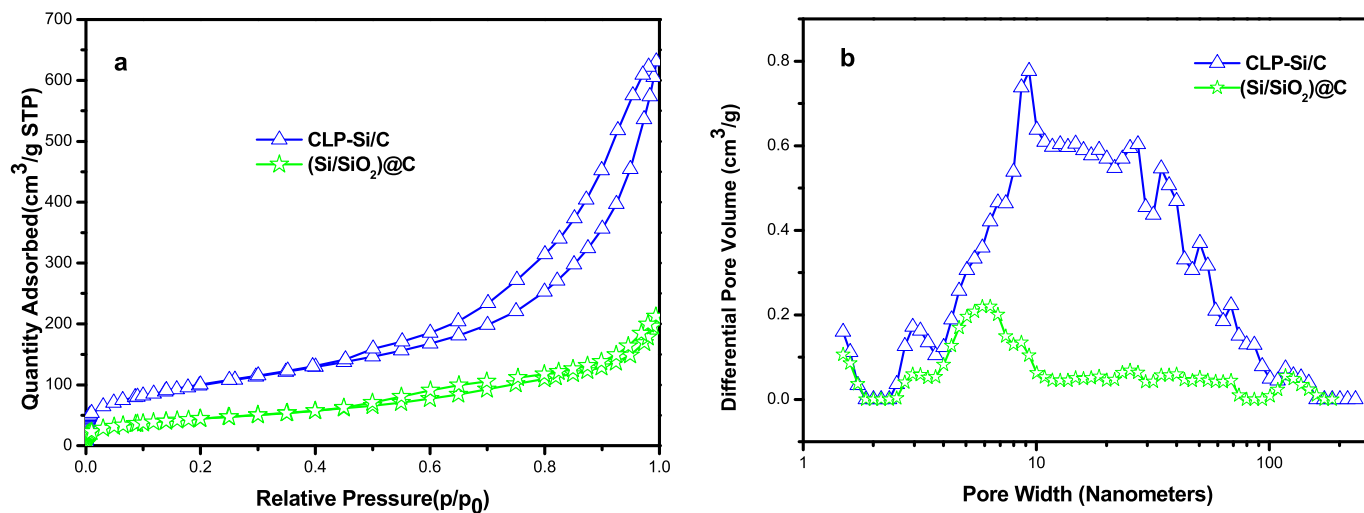


Fig. 5. (a) Nitrogen adsorption/desorption isotherms and (b) pore-size distribution curves using nonlocal density functional theory (NLDFT) of the sample without HF acid etching and CLP-Si/C sample.

Table 1

Specific surfaces area and porosity of the samples.

Sample	S_{total} ($m^2 g^{-1}$) ^a	V_{total} ($cm^3 g^{-1}$) ^b	$V_{micropores}$ ($cm^3 g^{-1}$) ^b	$V_{mesopores}$ ($cm^3 g^{-1}$) ^b	$V_{macropores}$ ($cm^3 g^{-1}$) ^b	APW (nm) ^c
DE	5.835	0.0023	0.0006	0.0015	0.0002	1.558
Si/SiO ₂ @C	159.798	0.1498	0.0065	0.1275	0.0158	8.227
CLP-Si/C	359.085	0.7436	0.0083	0.6613	0.0740	10.870

^a Total surface areas are derived using the multipoint Brunauer-Emmett-Teller (BET) method.

^b Total pore, micropore (<2 nm), mesopore (2–50 nm) and macropore (>50 nm) volume are derived using the nonlocal density functional theory ($D = 4 V/A$ by NLDFT).

^c Adsorption average pore width are derived using the multipoint Brunauer-Emmett-Teller method ($D = 4 V/A$ by BET).

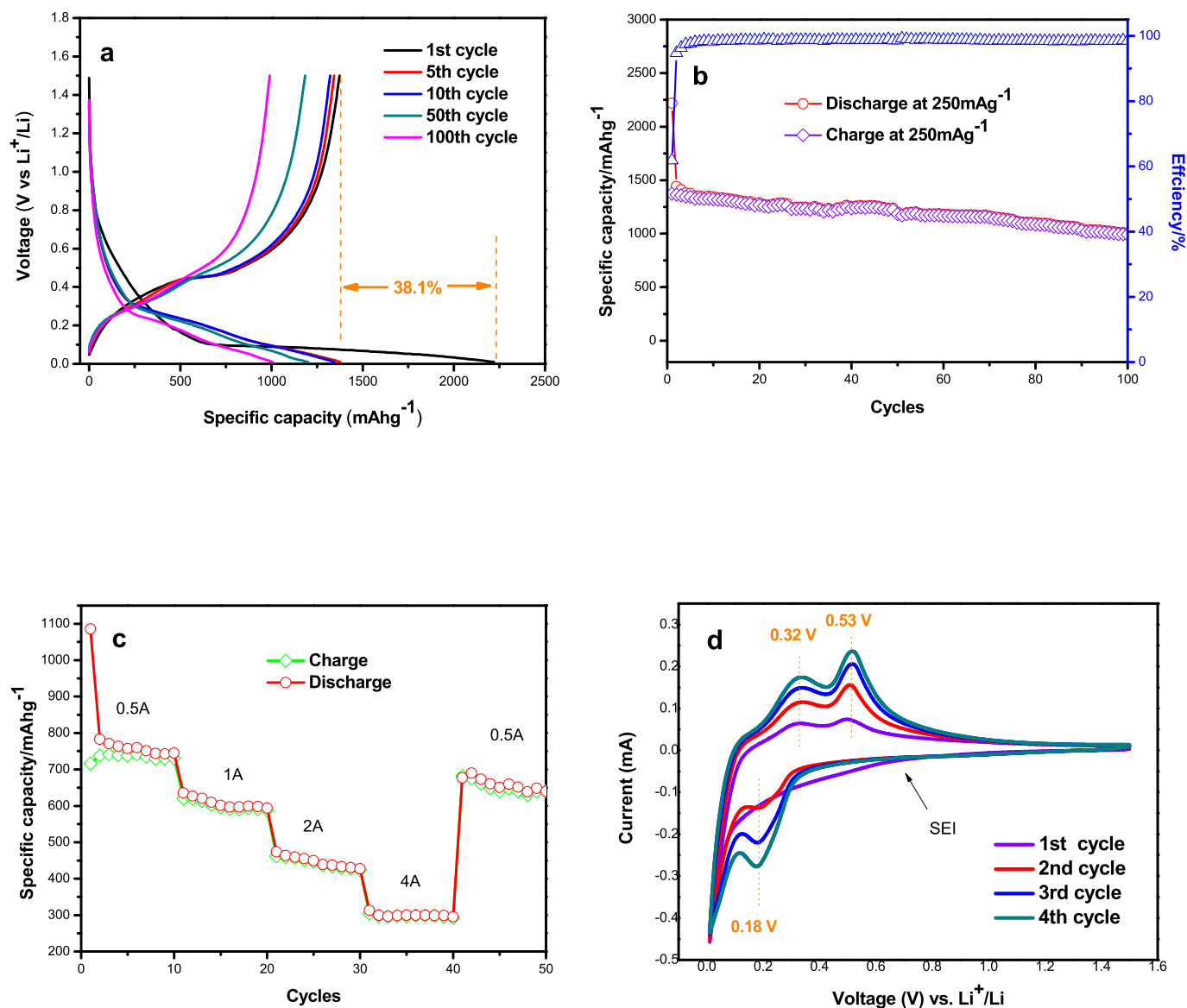


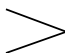
Fig. 6. Electrochemical performances of CLP-Si/C anode. (a) Discharge-charge curves at a current density of 0.25 A g⁻¹ between 0.01 and 1.5 V (vs. Li/Li⁺); (b) cycling performance at current density of 0.25 A g⁻¹ for 100 cycles; (c) rate capability at various current density from 0.5 to 4 A g⁻¹; (d) CV curves at a scan rate of 0.05 mV s⁻¹ in the voltage range of 0.01–1.5 V (vs. Li/Li⁺).

charge capacity of CLP-Si/C is 2219.1 and 1373.0 mAh g⁻¹ with an initial Coulomb efficiency (ICE) of 61.9%. The moderate ICE is probably associated with the large SSA of CLP-Si/C facilitating the generation of SEI film that consumes a part of Li⁺ [26,27]. Noticeably, this disadvantage in ICE can be overcome by the simple pre-lithiation [28,29]. The curve of the first discharge has a plateau below 0.10 V vs. Li/Li⁺, which generally requires a large polarization in the first cycle [30]. From the second cycle, the discharge platform is stabilized at 0.18 V vs. Li/Li⁺. Subsequently, the electrode was charged and Li⁺ ions were released from the Li_xSi. Fig. 6b shows cycling curve of CLP-Si/C electrodes at a rate of 250 mA g⁻¹. After 100 cycles, a reversible capacity of 990.6 mAh g⁻¹ is maintained and the capacity retention of CLP-Si/C anode is 72.1%. Rate capability of the CLP-Si/C anode was examined by continuous testing from 0.5 A g⁻¹ to 4.0 A g⁻¹ for 10 cycles and the results are shown in Fig. 6c. The average reversible capacity of anode at the corresponding current density is 733.8, 600.7, 442.8 and 297.6 mAh g⁻¹ in turns, once the current density is directly down to the initial

value of 0.5 A g⁻¹ from 4.0 A g⁻¹, the capacity of 650.2 mAh g⁻¹ is still kept. Electrochemical tests demonstrate that CLP-Si/C owns a satisfying capacity, cycling stability and rate performance as anode of LIB. Compared with previous reports, CLP-Si/C anode has certain advantages in reversible capacity and stability (as show in Table 2).

Fig. 6d shows CV of CLP-Si/C electrode in the potential range of 0.01–1.5 V with a scanning rate of 0.05 mV s⁻¹. At the first cycle, a broad cathodic peak appearing around 0.75 V could be attributed to the electrolyte decomposition and the concomitant formation of SEI films leading to the irreversible capacity of anode [31]. The intense peak locating from 0.13 to 0.01 V vs. Li/Li⁺ is assigned to Si lithiation process. The cathodic peaks around 0.18 V vs. Li/Li⁺ are corresponded to the Si lithiation process resulting in the formation of Li_xSi alloy. During the Si delithiation process, two anodic peaks at about 0.32 and 0.53 V vs. Li/Li⁺ could be assigned to the delithiation processes of alloys that are the phase transition from Li₁₅Si₄ to amorphous Li_xSi and subsequent transition from amorphous Li_xSi to Si [32]. The phenomenon indicates a kinetic enhancement

Table 2
Electrochemical performance of Si/C anode of LIB by using diatomite as precursor.

Sample	Current density	Number of Cycles	Initial capacity	Reversible capacity	References
Si/C	50 mA g ⁻¹	30	1628 mAh g ⁻¹	759 mAh g ⁻¹	Wang et al. [17],2012
Si/C	0.2 mA cm ⁻²	30	1818 mAh g ⁻¹	633 mAh g ⁻¹	Shen et al. [34],2012
Si/G	100 mA g ⁻¹	50	780 mAh g ⁻¹	600 mAh g ⁻¹	Zhang et al. [35],2017
Si/G	200 mA g ⁻¹	140	562 mAh g ⁻¹	460 mAh g ⁻¹	Guo et al. [36],2020
CLP-Si/C	250 mA g ⁻¹	50	1373 mAh g ⁻¹	1184 mAh g ⁻¹	 This Work
CLP-Si/C	250 mA g ⁻¹	100	1373 mAh g ⁻¹	991 mAh g ⁻¹	

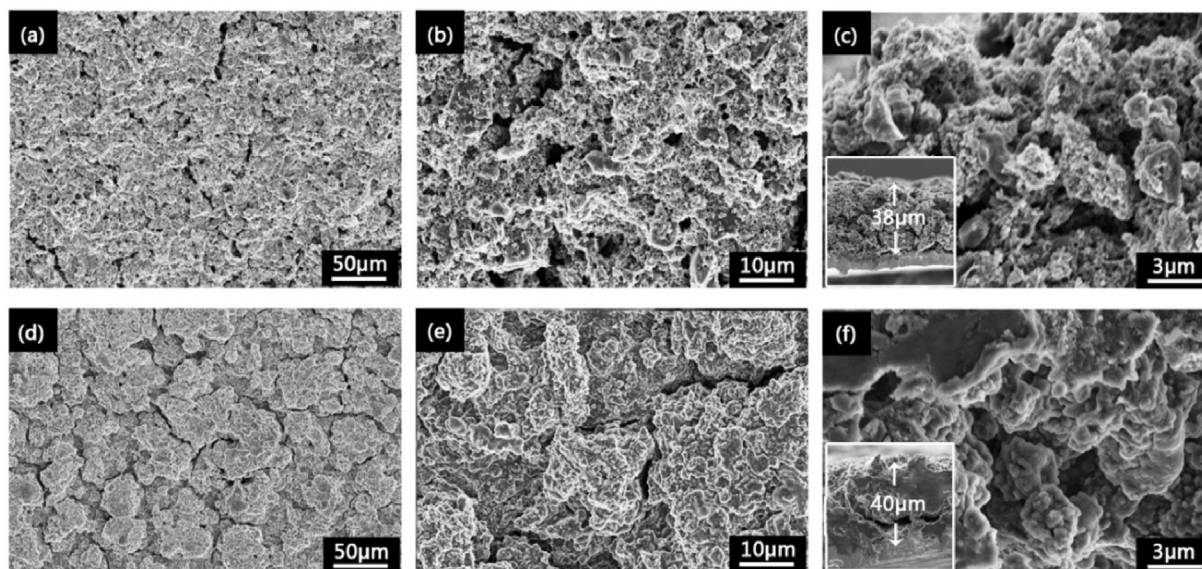


Fig. 7. SEM images of anode disk. (a) and (b) before cycling, (d) and (e) after 100 cycles, (c) and (f) cross-sectional observation before cycling and after 100 cycles at 0.25 A g⁻¹ (alloyed).

process of the CLP-Si/C anode before stabilization, which usually happens for the Si-based anodes [33].

The microstructure and morphology evolution of CLP-Si/C anode before and after the cycling tests were observed by using SEM and the results are shown in Fig. 7. Before the cycling tests, the surface of CLP-Si/C electrode appears uniform, smooth and a few cracks (Fig. 7a). After 100 cycles, the surface of electrode is slightly changed and the uniformly distributed shallow cracks can be observed possible due to the formation of SEI film and slight volume expansion of electrode, however, the integrity of the electrode is still maintained. Furthermore, SEM images of the cross-sectional view of electrodes show that the average thickness of active material well adhered to Cu current collector is 38.0 μm before the cycling test, after 100 cycles which is about 40 μm, which increases only about 5% in thickness. Compared to volumetric change of bulk Si (>300%), only a 5% increase in the electrode thickness even after 100 cycles well demonstrates the accommodation effect on volumetric change of Si by the CLP-Si/C.

4. Conclusions

By using a natural diatomite as both the precursor and self-template, a coral-like porous Si/C (CLP-Si/C) material has been successfully synthesized by the technology of MRR and acetylene CVD. CLP-Si/C owns a hierarchical pore structure of meso-/macropores that are inherited from diatomite itself, the unreacted SiO₂ in diatomite and MgO byproduct of MRR. Meanwhile CLP-Si/C is

constructed by a carbon shell and a porous nano-Si core. Hierarchical meso-/macropores and shell-core structure of CLP-Si/C materials can efficiently accommodate the volumetric effects of Si lithiation, there is only 5% increase in the thickness of active materials pasted on Cu collector after 100 charge-discharge cycles. Therefore, CLP-Si/C anode keep a reversible capacity of 990.6 mAh g⁻¹ at a rate of 250 mA g⁻¹ and exhibit a retention of 72% after 100 cycles. Since a good performance and the low cost of CLP-Si/C synthesized by using natural diatomite as precursor and template, the present work would contribute to develop the practical production and application of high-performance Si based anode materials in LIB.

CRediT authorship contribution statement

Fang Di: Conceptualization, Methodology, Data curation, Writing - original draft. **Ning Wang:** Methodology, Validation. **Lixiang Li:** Writing - review & editing, Project administration. **Xin Geng:** Validation, Supervision. **Haiming Yang:** Validation, Supervision. **Weimin Zhou:** Validation, Supervision. **Chengguo Sun:** Validation, Supervision. **Baigang An:** Conceptualization, Writing - review & editing, Project administration.

Declaration of competing interest

The authors declare that they have no known competing financial interests or personal relationships that could have

appeared to influence the work reported in this paper.

Acknowledgements

This work was financially supported by the National Natural Science Foundation of China project No. 51672117, 51672118, 51972156, 51872131, Distinguished Professor of Liaoning Province (2017) and Key Scientific Research Plan of Liaoning Province, No. 2018304017.

References

- [1] D. King, Global clean energy in 2017, *Science* 355 (2017), <https://doi.org/10.1126/science.aam7088>, 111–111.
- [2] H. Zhang, S. Liu, X. Yu, S. Chen, Improving rate capacity and cycling stability of Si-anode lithium ion battery by using copper nanowire as conductive additive, *J. Alloy, Compd* 822 (2020) 153664, <https://doi.org/10.1016/j.jallcom.2020.153664>.
- [3] M. Armand, J.M. Tarascon, Building better batteries, *Nature* 451 (2008) 652–657, <https://doi.org/10.1038/451652a>.
- [4] M.R. Palacin, Recent advances in rechargeable battery materials: a chemist's perspective, *Chem. Soc. Rev.* 38 (2009) 2565–2575, <https://doi.org/10.1039/b820555h>.
- [5] L.J. Fu, K. Endo, K. Sekine, T. Takamura, Y.P. Wu, H.Q. Wu, Studies on capacity fading mechanism of graphite anode for li-ion battery, *J. Power Sources* 162 (2006) 663–666, <https://doi.org/10.1016/j.jpowsour.2006.02.108>.
- [6] M.T. McDowell, S.W. Lee, W.D. Nix, Y. Cui, 25th anniversary article: understanding the lithiation of silicon and other alloying anodes for lithium-ion batteries, *Adv. Mater.* 25 (2013) 4966–4985, <https://doi.org/10.1002/adma.201301795>.
- [7] R. Teki, M.K. Datta, R. Krishnan, T.C. Parker, T.M. Lu, P.N. Kumta, N. Koratkar, Nanostructured silicon anodes for lithium ion rechargeable batteries, *Small* 5 (2009) 2236–2242, <https://doi.org/10.1002/smll.200900382>.
- [8] C.K. Chan, H. Peng, G. Liu, K. McIlwrath, X.F. Zhang, R.A. Huggins, Y. Cui, High-performance lithium battery anodes using silicon nanowires, *Nat. Nanotechnol.* 3 (2008) 31–35, <https://doi.org/10.1038/nnano.2007.411>.
- [9] X. Ding, X.X. Liu, Y. Huang, X. Zhang, Q. Zhao, X. Xiang, G. Li, P. He, Z. Wen, J. Li, Enhanced electrochemical performance promoted by monolayer graphene and void space in silicon composite anode materials, *Nanomater. Energy* 27 (2016) 647–657, <https://doi.org/10.1016/j.nanoen.2016.07.031>.
- [10] G. Zhu, Y. Gu, Y. Wang, Q. Qu, H. Zheng, Neuron like Si-carbon nanotubes composite as a high-rate anode of lithium ion batteries, *J. Alloys Compd.* 787 (2019) 928–934, <https://doi.org/10.1016/j.jallcom.2019.02.186>.
- [11] R. Ruffo, S.S. Hong, C.K. Chan, R.A. Huggins, Y. Cui, Impedance analysis of silicon nanowire lithium ion battery anodes, *J. Phys. Chem. C* 113 (2009) 11390–11398, <https://doi.org/10.1021/jp901594g>.
- [12] M.H. Park, M.G. Kim, J. Joo, K. Kim, J. Kim, S. Ahn, Silicon nanotube battery anodes, *Nano Lett.* 9 (2009) 3844–3847, <https://doi.org/10.1021/nl902058c>.
- [13] J.L. Gómez-Cámer, J. Morales, L. Sánchez, Anchoring Si nanoparticles to carbon nanofibers: an efficient procedure for improving Si performance in Li batteries, *J. Mater. Chem.* 21 (2010) 811–818, <https://doi.org/10.1039/c0jm01811b>.
- [14] M. Zhang, X.H. Hou, J. Wang, M. Li, S.J. Hu, Z.P. Shao, X. Liu, Interwoven Si@C/CNTs&CNFs composites as anode materials for Li-ion batteries, *J. Alloys Compd.* 588 (2014) 206–211, <https://doi.org/10.1016/j.jallcom.2013.10.160>.
- [15] Y. Yao, M.T. McDowell, I. Ryu, H. Wu, N. Liu, L. Hu, W.D. Nix, Y. Cui, Interconnected silicon hollow nanospheres for lithium-ion battery anodes with long cycle life, *Nano Lett.* 11 (2011) 2949–2954, <https://doi.org/10.1021/nl201470j>.
- [16] X. Li, P. Meduri, X. Chen, W. Qi, M.H. Engelhard, W. Xu, F. Ding, J. Xiao, W. Wang, C. Wang, J.G. Zhang, J. Liu, Interconnected silicon hollow nanospheres for lithium-ion battery anodes with long cycle life, *J. Mater. Chem.* 22 (2012) 11014–11017, <https://doi.org/10.1021/nl201470j>.
- [17] M.S. Wang, L.Z. Fan, M. Huang, J. Li, X. Qu, Conversion of diatomite to porous Si/C composites as promising anode materials for lithium-ion batteries, *J. Power Sources* 219 (2012) 29–35, <https://doi.org/10.1016/j.jpowsour.2012.06.102>.
- [18] Z. Wen, G. Lu, S. Cui, H. Kim, S. Ci, J. Jiang, P.T. Hurley, J. Chen, Rational design of carbon network cross-linked Si-SiC hollow nanosphere as anode of lithium-ion batteries, *Nanoscale* 6 (2014) 342–351, <https://doi.org/10.1039/c3nr04162j>.
- [19] L. Cheng, P. Liu, X.M. Chen, W.C. Niu, G.G. Yao, C. Liu, X.G. Zhao, Q. Liu, H.W. Zhang, Fabrication of nanopowders by high energy ball milling and low temperature sintering of Mg₂SiO₄ microwave dielectrics, *J. Alloys Compd.* 513 (2012) 373–377, <https://doi.org/10.1016/j.jallcom.2011.10.051>.
- [20] J. Wang, X. Meng, X. Fan, W. Zhang, H. Zhang, C. Wang, Scalable synthesis of defect abundant Si nanorods for high-performance Li-ion battery anodes, *ACS Nano* 9 (2015) 6576–6586, <https://doi.org/10.1021/acs.nano.5b02565>.
- [21] W. Luo, X. Chen, Y. Xia, M. Chen, L. Wang, Q. Wang, W. Li, J. Yang, Surface and interface engineering of silicon-based anode materials for lithium-ion batteries, *Adv. Energy Mater.* 7 (2017), <https://doi.org/10.1002/aenm.201701083>, 1701083.1–171701083.28.
- [22] X.H. Liu, J.Y. Huang, In situ TEM electrochemistry of anode materials in lithium ion batteries, *Energy Environ. Sci.* 4 (2011) 3844–3848, <https://doi.org/10.1039/c1ee01918j>.
- [23] X. Zuo, J. Zhu, P. Müller-Buschbaum, Y.J. Cheng, Silicon based lithium-ion battery anodes: a chronicle perspective review, *Nanomater. Energy* 31 (2017) 113–143, <https://doi.org/10.1016/j.nanoen.2016.11.013>.
- [24] Y. Yao, N. Liu, M.T. McDowell, M. Pasta, Y. Cui, Improving the cycling stability of silicon nanowire anodes with conducting polymer coatings, *Energy Environ. Sci.* 5 (2012) 7927–7930, <https://doi.org/10.1039/c2ee21437g>.
- [25] X. Zuo, Y. Xia, Q. Ji, X. Gao, S. Yin, M. Wang, X. Wang, B. Qiu, A. Wei, Z. Sun, Z. Liu, J. Zhu, Y.J. Cheng, Self-templating construction of 3D hierarchical macro-/mesoporous silicon from 0D silica nanoparticles, *ACS Nano* 11 (2017) 889–899, <https://doi.org/10.1021/acs.nano.6b07450>.
- [26] W.J. Zhang, A review of the electrochemical performance of alloy anodes for lithium-ion batteries, *J. Power Sources* 196 (2011) 13–24, <https://doi.org/10.1016/j.jpowsour.2010.07.020>.
- [27] J. Ryu, D. Hong, S. Choi, S. Park, Synthesis of ultrathin Si nanosheets from natural clays for lithium-ion battery anodes, *ACS Nano* 10 (2016) 2843–2851, <https://doi.org/10.1021/acs.nano.5b07977>.
- [28] N.A. Liu, L.B. Hu, M.T. McDowell, A. Jackson, Y. Cui, Prelithiated silicon nanowires as an anode for lithium ion batteries, *ACS Nano* 5 (2011) 6487–6493, <https://doi.org/10.1021/nn2017167>.
- [29] J. Liu, P. Kopold, P.A. Aken, J. Maier, Y. Yu, Energy storage materials from nature through nanotechnology: a sustainable route from reed plants to a silicon anode for Lithium-ion batteries, *Angew. Chem.* 127 (2015) 9768–9772, <https://doi.org/10.1002/ange.201503150>.
- [30] X. Zhou, Y.X. Yin, L.J. Wan, Y.G. Guo, Facile synthesis of silicon nanoparticles inserted into graphene sheets as improved anode materials for lithium-ion batteries, *Chem. Commun.* 48 (2012) 2198–2200, <https://doi.org/10.1039/c2cc17061b>.
- [31] D.T. Ngo, H.T.T. Le, X.M. Pham, J.W. Jung, N.H. Vu, J.G. Fisher, W.B. Im, I.D. Kim, C.J. Park, Highly porous coral-like silicon particles synthesized by an ultra-simple thermal-reduction method, *J. Mater. Chem.* 6 (2018) 2834–2846, <https://doi.org/10.1039/C7TA09042K>.
- [32] J. Zhu, J. Yang, Z. Xu, J. Wang, Y. Nuli, X. Zhuang, X. Feng, Silicon anodes protected by a nitrogen-doped porous carbon shell for high-performance lithium-ion batteries, *Nanoscale* 9 (2017) 8871–8878, <https://doi.org/10.1039/c7nr01545c>.
- [33] L. Shen, X. Guo, X. Fang, Z. Wang, L. Chen, Magnesiumthermally reduced diatomaceous earth as a porous silicon anode material for lithium ion batteries, *J. Power Sources* 213 (2012) 229–232, <https://doi.org/10.1016/j.jpowsour.2012.03.097>.
- [34] Y. Zhang, H. Chu, L. Zhao, L. Yuan, Si/graphene composite as high-performance anode materials, *J. Mater. Sci. Mater. Electron.* 28 (2017) 1–7, <https://doi.org/10.1007/s10854-017-6357-0>.